Hydrogenated Amorphous Silicon Thin Film Solar Cells Using a Hybrid Buffer Layer of Gold Nanoparticle and Tungsten Oxide Thin Film

Kyoung Soo Yook, Min Seung Choi, Dong Ho Kim, Chang Su Kim, Myung Kwan Song, Jae Wook Kang, Jung Dae Kwon, Youngsoo Jeong, Kee Seok Nam, Sung Hun Lee, Hyung Hwan Jung, Kwun Bum Chung, Tae-Sung Bae, Jun Yeob Lee and Seung Yoon Ryu

ECS Solid State Lett. 2012, Volume 1, Issue 5, Pages Q42-Q44.
doi: 10.1149/2.009205ssl

ECS Solid State Letters, **1** (5) Q42-Q44 (2012)
2162-8742/2012/1(5)/Q42/3/$28.00 © The Electrochemical Society

Hydrogenated Amorphous Silicon Thin Film Solar Cells Using a Hybrid Buffer Layer of Gold Nanoparticle and Tungsten Oxide Thin Film

Kyoung Soo Yook,[a] Min Seung Choi,[b] Dong Ho Kim,[b] Chang Su Kim,[b] Myung Kwan Song,[b] Jae Wook Kang,[b] Jung Dae Kwon,[b] Youngsoo Jeong,[b] Kee Seok Nam,[b] Sung Hun Lee,[b] Hyung Hwan Jung,[b,c] Kwun Bum Chung,[c] Tae-Sung Bae,[d] Jun Yeob Lee,[a,z] and Seung Yoon Ryu[b,z]

[a]*Department of Polymer Science and Engineering, Dankook University, Yongin-City, Gyeonggi-Do 448-701, Korea*
[b]*Advanced Functional Thin Films Department, Korea Institute of Materials Science (KIMS), Changwon 641-831, Korea*
[c]*Department of Physics, Dankook University, Anseo-Dong, Chonan 330-714, Korea*
[d]*Korea Basic Science Institute, Jeonju, Jeonbuk 561-756, Korea*

A double layer of gold nano particles (Au-NPs) and amorphous tungsten oxide (a-WO_3) was employed as a buffer layer on textured fluorine-tin oxide (FTO) glass in *pin*-type hydrogenated amorphous silicon solar cells (a-Si:H SCs). Au-NPs of ~10 nm size were spin coated and a-WO_3 layer was thermally evaporated between Au-NPs on a FTO glass and hydrogenated amorphous *p*-type Si layer. a-Si:H SCs with a double buffer layer showed higher efficiency of 7% improvement, 8.059% from a value of 7.530%, and increased current density of 8.3% improvement, 14.212 mA/cm^2 from a value of 13.120 mA/cm^2, originating from the enhancement of electrical interface contact and bandgap alignment, as well as the slight absorption and surface plasmon resonance effect due to Au-NPs on textured FTO glass.
 [DOI: 10.1149/2.009205ssl]

Manuscript submitted April 4, 2012; revised manuscript received July 10, 2012. Published August 29, 2012.

Due to their low fabrication cost, *pin*-type hydrogenated amorphous silicon solar cells (a-Si:H SCs) are potential renewable solar energy sources.[1–9] However, the device efficiency of a-Si:H SCs is still lower than that of poly-Si SCs. One method of improving device performances in a-Si:H SCs is to insert a transition metal oxide, such as tungsten oxide (WO_3),[2,3,10] between a textured fluorine-tin oxide (FTO) glass and a *p*-type Si layer as an adjusted *p*-type electrode. The WO_3 layer increases carrier collection[10] due to the band alignment between neighboring layers in a-Si:H SCs[2,3] and provides a large shunt resistance, which reduces carrier recombination at the interface.[10]

The addition of highly conducting gold nano-particles (Au-NPs) can also improve a-Si:H SC performance through light trapping and out-coupling through a surface plasmonic resonance (SPR) effect.[1,7–9,11–14] Furthermore, the FTO / Au-NP interface reduces electrical contact resistance and, optimizes energy level alignment, which in turn adjusts the work-function, enhancing the movement of hole carriers.[15] However, metals or metal NPs can induce recombination defect sites at the interface with the Si layer, resulting in device degradation.[7–9,14] Moreover, the SPR effect from Au-NPs has been observed usually in organic solar cells with a flat indium tin oxide (ITO), rather than a textured FTO, electrode.[1,7–9,11–13]

For this reason, a-Si:H SCs with a double buffer layer of Au-NPs / WO_3 on textured FTO glass, in which WO_3 is used as both a dipole layer and a capping layer, is proposed. WO_3[2,3,10] is used as a window layer due to its wide optical band-gap, making it particularly suitable for the high valence band of *p*-type Si layers. Although Si-based devices show reasonable efficiencies of 6~7% without any buffer layer, double interfacial layers can further improve device performance in a-Si:H SCs.[1–6]

Experimental

In this paper, we present a study on how the WO_3 capping layer can influence the device characteristics of a superstrate a-Si SCs. First, FTO glass was cleaned with deionized water, acetone, and isopropanol under sonication. A superstrate device structure with a double buffer layer was prepared by spin coating aqueous solution of ~10 nm Au-NPs at a speed of 2000 rpm followed by thermal evaporation of a 4 nm thick WO_3 layer. All Au-NPs solution had approximately 0.01% $HAuCl_4$ suspended in 0.01% tannic acid with 0.04% trisodium citrate, 0.26 mM potassium carbonate, and 0.02% sodium azide as a preservative. (Sigma Aldrich; products number is G 1527) The spin coated Au-NP layer was baked on a hot plate at 200 °C. After WO_3 deposition, *pin* amorphous Si layers (*p* layer / intrinsic layer / *n* layer: 12 nm / 450 nm / 25 nm) were consecutively deposited using plasma enhanced chemical vapor deposition. Finally, silver metal (150 nm) was deposited by thermal evaporation using a shadow mask with the area of 0.25 cm^2. Current density-voltage (*J-V*) characteristics were measured using a Keithley 2400 source meter under 100 mW/cm^2 (AM 1.5G) irradiation from a solar simulator.

Results and Discussion

The superstrate a-Si:H SC structure and band diagram are shown in Fig. 1a and 1b,[2] respectively. The band alignment between Au-NPs and WO_3 films match well for better movement of hole carriers between the FTO glass and the *p*-type Si layer. Fig. 1c shows a micrograph of Au-NPs on textured FTO glass using an Ultra High Resolution Field Emission Scanning Electron Microscope (UHR FE-SEM, S-5500, Hitachi, Japan) installed in the KBSI Jeonju Center at an accelerating voltage of 7 kV.

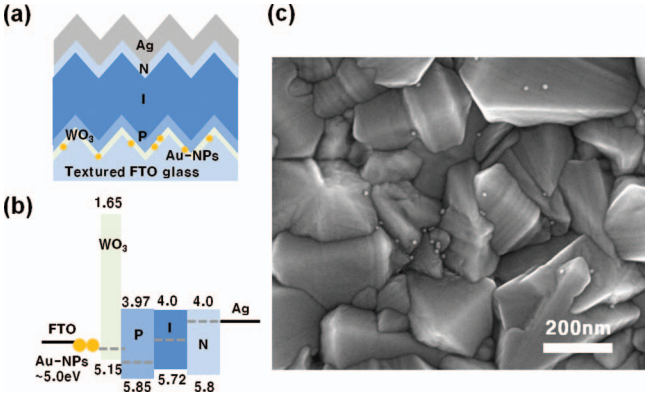

Figure 1. (a) Schematic device structure and (b) band diagram of solar cells with various buffer layers, including a Au-NP / WO_3 double buffer layer, (c) UHR FE-SEM image of spin-coated (2000 rpm) Au-NPs (~10 nm) on textured FTO glass.

[z]E-mail: justie74@kims.re.kr; leej17@dankook.ac.kr

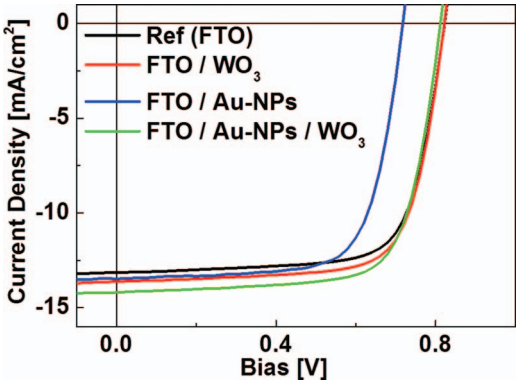

Figure 2. The *J-V* characteristics (J_{sc}) of solar cells with various buffer layers, including a WO_3 single buffer layer, a Au-NP single buffer layer, and a Au-NP / WO_3 double buffer layer.

The *J-V* characteristics, and short-circuit current (J_{sc}), of four kinds of a-Si:H SC devices are shown in Fig. 2. The device characteristics of *pin* type a-Si:H SCs were improved with a 4 nm thickness of WO_3 and a Au-NP / WO_3 double buffer layer, compared to a reference device, due to the electrical Schottky barrier model[1,2,9] and the slight SPR effect of Au-NPs.[1,7–9,11–14] The device performance was the best when a 4 nm thickness of WO_3 was chosen, comparing to 2 nm and 8 nm, relatively. (data not shown) A 4 nm thick WO_3 might not be able to cover 10 nm-size Au-NPs sufficiently. The complicated optical and electrical situation might happen and it is hard to explain the exact mechanism due to incomplete coverage. However, thin WO_3 has been used in many other groups, and they did not also suggest any proof of thin WO_3 mophology.[2–5,10]

The improved device characteristics can be explained by the transmittance and reflectivity data in Fig. 3. The total transmittance and reflectivity of FTO glass, in the integral-sphere due to the textured FTO, are quite similar for a single WO_3 layer and an Au NP / WO_3 double buffer layer, but J_{sc} of the Au-NP / WO_3 double buffer layer device increases relative to that of the device with only a single WO_3 layer. J_{sc} was enhanced from the better electrical interface contact and bandgap alignment, as well as device physics between FTO and *p*-type a-Si:H layer, and the slight SPR effect due to the small Au-NPs.[1,7–9,11–14] Interestingly, the J_{sc} of the device with only Au-NPs was also increased due to the better electrical contact and the slight SPR effect, but the open circuit-voltage (V_{oc}) was severely degraded by direct contact between Au-NPs and the p-type a-Si:H layer,[7–9,14] which can be explained by the impedance data in Fig. 4b. The impedance[16,17] of the device with only a Au-NP single layer showed the lowest value, since the electrical field will tend to be focused around the Au-NPs.

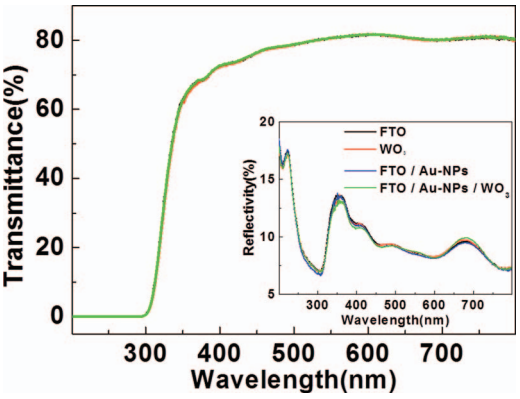

Figure 3. The transmittance of a textured FTO glass with a WO_3 single buffer layer, Au-NP single buffer layer, and a Au-NP / WO_3 double buffer layer. The inset shows the reflectivity data.

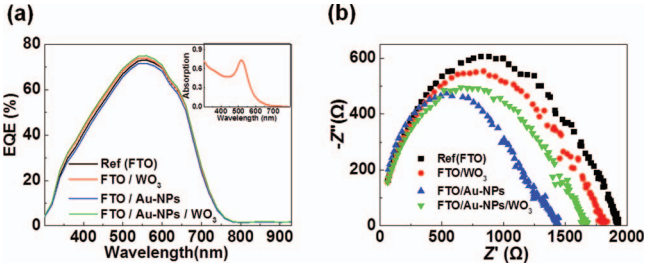

Figure 4. (a) The EQE and (b) impedance data of devices with a WO_3 single buffer layer, a Au-NP single buffer layer, and a Au-NP / WO_3 double buffer layer. The inset in (a) shows the absorption data of Au-NPs (10 nm) in solution.

In addition, the V_{oc} of the device with only an Au-NP single layer decreased due to Ohm's law.

This enhancement of the device current density was also confirmed by measuring the external quantum efficiency (EQE). Fig. 4a shows EQE curve of a-Si SCs with different buffer layer structures. The EQE was high around 560 nm in the a-Si:H SC with a double buffer layer, indicating that Au-NPs induce slight surface plasmons and thus absorption and SPR effects at the interface between FTO and WO_3. The presence of slight surface plasmons was confirmed through measurements of the absorption of Au-NPs in water-based solution at inset in Fig. 4a, showing a redshift from 520 nm to 560 nm due to the different environmental dielectric constant.[11] The coherent collective oscillation of conduction electrons happened surrounding the metallic surfaces.[13] The excitation peak is induced when the frequency of the incident light matched its resonance peak, resulting in unique optical properties, the dielectric environment of Au-NPs, and also, size, shape of NPs.[13] This redshift is ascribed to the different dielectric constant between 20[18] of WO_3 and 78.54 of water-based Au-NPs at room temperature. Surface plasmons and absorption effects enhanced the absorption of the a-Si light absorbing layer, resulting in the increase of J_{sc}.

The effect of WO_3 and Au-NP / WO_3 buffer layers on the resistance at the interface was investigated through impedance measurements. Figure 4b shows the influence of the Au-NP / WO_3 double buffer layer on the impedance. The device with only a WO_3 single buffer layer showed lower impedance than the reference device, indicating that the WO_3 single layer acted as a dipole layer, reducing the potential barrier and interfacial impedance between FTO and the *p*-type Si layer. The device with an Au-NP / WO_3 double buffer layer was better than the other devices, indicating that Au-NPs improved performance through a lower resistance at the FTO/WO_3 interface, in addition to slight absorption and SPR effects from plasmonic theory.

Table I shows the characteristics of four kinds of devices and reveals that the a-Si:H SC with a Au-NP / WO_3 double buffer layer shows the highest device efficiency of 8.059%, mainly due to a high J_{sc}, increased from 13.120 mA/cm^2 to 14.212 mA/cm^2, in which the enhancement ratio is as much as ~8%. The fill factor (FF) is almost same, around 0.716. Many researchers have shown that Au-NPs can be used to induce the SPR effect, including near field interference with neighboring particles with sizes between 50 nm and 100 nm, and scattering effects over long distances between NPs over 100 nm.[7–9,11–14] However, Au-NPs of 10 nm were used in this

Table I. Photovoltaic performance of a-Si solar cells with various buffer layers, a WO_3 single buffer layer, an Au-NP single buffer layer, and an Au-NP / WO_3 double buffer layer.

	Eff (%)	J_{sc} (mA/cm^2)	V_{oc} (Voltage)	FF
Ref (FTO)	7.530	13.120	0.796	0.720
FTO / WO_3	7.787	13.552	0.801	0.716
FTO / Au-NPs	7.156	13.453	0.745	0.713
FTO / Au-NPs / WO_3	8.059	14.212	0.791	0.716

work and only slight absorption effect was enhanced, not scattering effect.[1,7–9,11–14] Moreover, the current density of devices with only a WO_3 single buffer layer was higher than that of the reference device, likely due to the reduced the potential barrier between FTO and the *p*-type a-Si:H layer from the WO_3 layer. However, even though the Au-NP size is around 10 nm, the current density of a device using an Au-NP / WO_3 double buffer layer was higher than that for devices with only a WO_3 single buffer layer. The higher current density could be attributed to the better electrical contact and slight absorption and SPR effects from Au-NPs and the capping effect from WO_3, which blocks defect sites between Au-NPs and the p-type A-Si layer.[7–9,14]

Conclusions

In summary, we have fabricated superstrate *pin* a-Si:H SCs utilizing a Au-NP / WO_3 double buffer layer between the FTO and the *p*-type Si layer. We investigated how the WO_3 capping layer to Au-NPs on textured FTO glass can influence device characteristics of a-Si solar cells. The observed current density-dependent device characteristics show that a WO_3 capping layer with Au NPs might lead to the development of more efficient and stable a-Si solar cells.

Acknowledgment

The present research was supported by the research fund (2012-PNK2860) of the Korea Institute of Materials Science, a subsidiary branch of the Korea Institute of Machinery and Materials. J.Y.Lee acknowledges financial support from GRRC program of Gyeonggi Province (GRRC Dankook2012-B01: Development of High Efficiency White OLED Materials and Their Devices), collaborative R&D program with technology advanced country (2011-advanced-B-105) and IT R&D program of MKE/KEIT [KI002104-2010-02]. Authors Kyoung Soo Yook and Min Seung Choi contributed equally to this paper.

References

1. J. M. Lee, S. J. Yun, J. K. Kim, and J. W. Lim, *Electrochem. Solid-State Lett.*, **14**, B124 (2011).
2. L. Fang, S. J. Baik, K. S. Lim, S. H. Yoo, M. S. Seo, S. J. Kang, and J. W. Seo, *Appl. Phys. Lett.*, **96**, 193501 (2010).
3. L. Fang, S. J. Baik, J. W. Kim, S. J. Kang, J. W. Seo, J. W. Jeon, Y. H. Kim, and K. S. Lim, *J. Appl. Phys.*, **109**, 104501 (2011).
4. S. J. Baik and K. S. Lim, *J. Appl. Phys.*, **109**, 084506 (2011).
5. S. J. Baik and K. S. Lim, *Journal of Korean Physical Society*, **59**, 443 (2011).
6. S. J. Baik, S. J. Kang, and K. S. Lim, *Appl. Phys. Lett.*, **97**, 122102 (2010).
7. S. Pillai, K. R. Catchpole, T. Trupke, and M. A. Green, *J. Appl. Phys.*, **101**, 093105 (2007).
8. M. Losurdo, M. M. Giangregorio, G. V. Bianco, A. Sacchetti, P. Capezzuto, and G. Bruno, *Solar Energy Materials & Solar Cells*, **93**, 1749 (2009).
9. D. Derkacs, S. H. Lim, P. Matheu, W. Mar, and E. T. Yu, *Appl. Phys. Lett.*, **89**, 093103 (2006).
10. S. C. Han, W. S. Shin, M. S. Seo, D. Gupta, S. J. Moon, and S. H. Yoo, *Organic Electronics*, **10**, 791 (2009).
11. J. Yang, J. You, Chun-Chao Chen, Wan-Ching Hsu, Hai-ren Tan, X. W. Zhang, Z. Hong, and Y. Yang, *ACS Nano*, **5**, 6210 (2011).
12. D. H. Wang, D. Y. Kim, K. W. Choi, J. H. Seo, S. H. Im, J. H. Park, O. O. Park, and A. J. Heeger, *Angew. Chem. Int. Ed.*, **50**, 5519 (2011).
13. Jyh-Lih Wu, Fang-Chung Chen, Yu-Sheng Hsiao, Fan-Ching Chien, P. Chen, Chun-Hong Kuo, M. H. Huang, and Chain-Shu Hsu, *ACS Nano*, **5**, 959 (2011).
14. H. A. Atwater and A. Polman, *Nat. Mater.*, **9**, 205 (2010).
15. J. C Bernede, L. Cattin, M. Morsli, and Y. Berredjem, *Solar Energy Materials & Solar Cells*, **92**, 1508 (2008).
16. T. Kuwabara, Y. Kawahara, T. Yamaguchi, and K. Takahashi, *ACS Applied. Materials. & Interfaces*, **1**, 2107 (2009).
17. B. J. Leever, C. A. Bailey, T. J. Marks, M. C. Hersam, and M. F. Durstock, *Adv. Energy Mater.*, **2**, 120 (2012).
18. S. K. Deb, *Philos. Mag.*, **27**, 801 (1973).